



**HAL**  
open science

# The recruitment of indirect waves within primary motor cortex during motor imagery: A directional transcranial magnetic stimulation study

Cécilia Neige, Valentin Ciechelski, Florent Lebon

## ► To cite this version:

Cécilia Neige, Valentin Ciechelski, Florent Lebon. The recruitment of indirect waves within primary motor cortex during motor imagery: A directional transcranial magnetic stimulation study. *European Journal of Neuroscience*, 2022, 56 (12), pp.6187-6200. 10.1111/ejn.15843 . hal-04011465

**HAL Id: hal-04011465**

**<https://hal.science/hal-04011465>**

Submitted on 2 Mar 2023

**HAL** is a multi-disciplinary open access archive for the deposit and dissemination of scientific research documents, whether they are published or not. The documents may come from teaching and research institutions in France or abroad, or from public or private research centers.

L'archive ouverte pluridisciplinaire **HAL**, est destinée au dépôt et à la diffusion de documents scientifiques de niveau recherche, publiés ou non, émanant des établissements d'enseignement et de recherche français ou étrangers, des laboratoires publics ou privés.

1     **The recruitment of indirect-waves within primary motor cortex during**  
2     **motor imagery: A directional Transcranial Magnetic Stimulation study**

3  
4     **Running title:** Using directional TMS during motor imagery

5  
6  
7                   Cécilia Neige<sup>1,§</sup>, Valentin Ciechelski<sup>1</sup> & Florent Lebon<sup>1</sup>

8  
9     <sup>1</sup> INSERM UMR1093-CAPS, Université Bourgogne Franche-Comté, UFR des Sciences du Sport, F-  
10  21078, Dijon, France.

11     <sup>§</sup> *current address:* PSYR<sup>2</sup> Team, Centre Hospitalier Le Vinatier, INSERM U1028/CNRS UMR5292,  
12  Lyon Neurosciences Research Center, Université Claude Bernard Lyon 1, F-69000, Bron, France.

13  
14     **Corresponding Author:**

15     Cécilia Neige, Université de Bourgogne Franche-Comté, Dijon, Campus Universitaire, UFR STAPS,  
16     BP 27877, F-21078 Dijon, France.

17     cecilia.neige@inserm.fr, Tel.: +333 80396754, Fax: +333 80396749

18  
19     **Word counts:** 5861 words

20  
21     **Acknowledgments**

22  
23     This research was financially supported by the ‘Investissements d’Avenir’ French program,  
24     project ISITE-BFC (contract ANR-15-IDEX-0003).

25     Cécilia Neige: Conceptualization, Methodology, Investigation, Formal analysis,  
26     Visualization, Writing -Original draft preparation.

27     Valentin Ciechelski: Investigation, Formal analysis.

28     Florent Lebon: Conceptualization, Data curation, Supervision, Funding acquisition, Writing -  
29     Review & Editing.

30     The authors want to thank Dr. Anaïs Gouteron for participant’s medical inclusion, William  
31     Dupont and Dylan Rannaud Monany for technical assistance during acquisition of data.

32 **Abstract**

33 Motor imagery (MI) refers to the mental simulation of an action without overt movement.  
34 While numerous transcranial magnetic stimulation (TMS) studies provided evidence for a  
35 modulation of corticospinal excitability and intracortical inhibition during MI, the neural  
36 signature within the primary motor cortex is not clearly established. In the current study, we  
37 used directional TMS to probe the modulation of the excitability of early and late indirect-  
38 waves (I-waves) generating pathways during MI. Corticospinal responses evoked by TMS  
39 with posterior-anterior (PA) and anterior-posterior (AP) current flow within the primary  
40 motor cortex evoke preferentially early and late I-waves, respectively. Seventeen participants  
41 were instructed to stay at rest or to imagine maximal isometric contractions of the right flexor  
42 carpi radialis. We demonstrated that the increase of corticospinal excitability during MI is  
43 greater with PA than AP orientation. By using paired-pulse stimulations, we confirmed that  
44 short-interval intracortical inhibition (SICI) increased during MI in comparison to rest with  
45 PA orientation, whereas we found that it decreased with AP orientation. Overall, these results  
46 indicate that the pathways recruited by PA and AP orientations that generate early- and late I-  
47 waves are differentially modulated by MI.

48

49

50

51 **Key words:** Primary motor cortex, adaptive threshold-hunting, motor-evoked potentials, short  
52 interval intracortical inhibition, corticospinal excitability.

53

## 54 **Introduction**

55 Motor imagery (MI) is a cognitive process that refers to the mental simulation of an action  
56 without overt movement (Jeannerod & Decety, 1995). MI is known to activate brain regions  
57 also involved during motor execution but is accompanied by a voluntary inhibition of the  
58 actual movement (Decety, 1996). Using vascular space occupancy method combined with  
59 high-resolution (7T) functional magnetic resonance imaging, Persichetti et al. (2020)  
60 supported the idea that MI activated only the superficial layers II/III of the primary motor  
61 cortex (M1) with cortico-cortical connections from somatosensory and premotor areas (Huber  
62 *et al.*, 2017). In contrast, actual finger movements activated both superficial layers and the  
63 deeper layers Vb/VI in M1 with descending excitatory corticospinal projections. These results  
64 would nicely explain the absence of muscle activity during MI. However, this exclusive  
65 activation of superficial layers within M1 during MI is at odds with numerous observations in  
66 the current literature. Indeed, past studies using different methodological approaches found  
67 neural modulations downstream of the pyramidal cells while imagining (Li *et al.*, 2004;  
68 Grosprêtre *et al.*, 2015). For example, by using a combination of different techniques during  
69 MI, Grosprêtre et al. (2015) provided evidence for a subliminal motor output that traveled  
70 along the corticospinal tract and reached the spinal level but did not activate alpha-  
71 motoneurons. These modulations following motor imagery practice, besides the changes  
72 within M1, would also explain the improvement in motor learning (Ruffino *et al.*, 2017).

73 Transcranial magnetic stimulation studies (TMS) provided evidence of the activation of the  
74 corticospinal pathway during MI, compared to rest (Yahagi & Kasai, 1999; Grosprêtre *et al.*,  
75 2016). This activation is classically marked by an increase in the amplitude of the motor  
76 evoked potentials (MEPs) evoked by single-pulse TMS and recorded in the specific muscle  
77 involved in the imagined movement (Yahagi & Kasai, 1999; Lebon *et al.*, 2012; Grosprêtre *et*  
78 *al.*, 2016; Neige *et al.*, 2020, 2021). According to Di Lazzaro and Ziemann (2013), the axons  
79 of the more superficial pyramidal neurons (P2/P3) are conceivably the most excitable neural  
80 elements to low-threshold TMS, due to their location close to the stimulating coil. Moreover,  
81 these axons also represent the primary source of excitatory descending input to pyramidal  
82 tract neurons of layer V (Anderson *et al.*, 2010). Therefore, if TMS activates axons of  
83 superficial layer cells preferentially and MI induces an increase in TMS-evoked responses, it  
84 is most likely that superficial pyramidal neurons activated during MI directly excite deeper  
85 layers, contradicting the findings by Persichetti et al. (2020).

86 Previous studies that used TMS during MI rely on interpreting the MEPs amplitude evoked by  
87 the posterior-anterior (PA) current direction. However, MEPs amplitude is a complex and  
88 global readout that is thought to reflect the summation of several monosynaptic and  
89 polysynaptic descending inputs, termed D- (direct) and I-(indirect) waves, as evidenced from  
90 spinal epidural recordings (Di Lazzaro *et al.*, 2012). The first descending volley is thought to  
91 originate from direct activation (D-wave) of corticospinal tract axons, whereas the latter I-  
92 waves are thought to derive from indirect, trans-synaptic activation of the corticospinal  
93 neurons (Di Lazzaro & Rothwell, 2014; Ziemann, 2020). These I-waves usually appear at ~  
94 1.2–1.5 ms intervals are numbered in order of their appearance, and are referred to as either  
95 early (I1) or late (I2, I3, I4) I-waves (Di Lazzaro *et al.*, 2012; Ziemann, 2020). The directional  
96 TMS technique is a non-invasively and valuable approach used to activate distinct sets of  
97 synaptic inputs to corticospinal neurons responsible for the early and late I-waves pathway. It  
98 has been proposed that TMS-induced electric currents flowing from LM (latero-medial), PA  
99 and AP (anterior to posterior) directions activate different sets of excitatory synaptic inputs  
100 that arrive at the pyramidal tract neurons several milliseconds apart (Di Lazzaro & Rothwell,  
101 2014; Di Lazzaro *et al.*, 2017). LM stimulation at high intensity can directly activate the  
102 corticospinal axons of pyramidal tract neurons, evoking a short-latency D-wave (Di Lazzaro  
103 & Rothwell, 2014). PA stimulation preferentially elicits primarily early I-wave, which is  
104 thought to originate from excitatory inputs to the basal dendrites of the corticospinal neurons  
105 in layer V of M1 (Di Lazzaro & Ziemann, 2013; Hannah, 2020). AP stimulation preferentially  
106 elicits later and more dispersed I-waves which are thought to result from mono- and poly-  
107 synaptic inputs from layers II/III of M1 (Ziemann, 2020), as well as the activation of  
108 horizontal cortico-cortical connections from surrounding brain regions to M1 (Di Lazzaro *et*  
109 *al.*, 2017; Hannah, Cavanagh, *et al.*, 2018). Therefore, comparing MEPs amplitude recorded  
110 in hand muscles induced by PA and AP current directions allows us to infer the different I-  
111 wave contributions evoked by separate subpopulations of interneurons. To our knowledge,  
112 whether MI differentially modulates specific circuits with each current direction remains  
113 unexplored. As MI is an important field of research in cognitive neuroscience and motor  
114 rehabilitation, it is important to decipher the neural circuits underlying imagined movements.

115 In the current study, we investigated the modulation of early and late I-waves generating  
116 pathways specifically activated by PA and AP-directed currents during MI and rest  
117 conditions. We used single-pulse and paired-pulse TMS to probe corticospinal excitability  
118 and short-interval intracortical inhibition (SICI). Interestingly, SICI affects mainly later I-

119 waves that are mainly targeted by AP orientation (Nakamura *et al.*, 1997; Hanajima *et al.*,  
120 1998; Cirillo & Byblow, 2016; Wessel *et al.*, 2019), and SICI increases during MI but is only  
121 observed with PA orientation (Neige *et al.*, 2020).

122 If MI preferentially recruits superficial layers within M1 (Persichetti *et al.*, 2020), we would  
123 observe a greater increase in corticospinal excitability and SICI with AP than with PA  
124 orientation. On the contrary, if MI activates neural circuits downstream of the pyramidal cells  
125 (Grosprêtre *et al.*, 2015), we expect that MI would induce a specific modulation of the  
126 pathway recruited by PA orientation that preferentially generates early I-wave. This pathway  
127 would be critical in modulating both corticospinal excitability and SICI.

## 128 **Material and Methods**

### 129 **Participants**

130 Seventeen healthy volunteers were recruited in the current study after providing written  
131 informed consent (3 females; age = 24.3 years, range 21-31 years; height =  $177 \pm 8$  cm;  
132 weight =  $69 \pm 10$  kg; right-handed as assessed by the Edinburgh Handedness Inventory  
133 (Oldfield, 1971)). All volunteers were screened by a medical doctor for contraindications to  
134 TMS (Rossi *et al.*, 2009). The protocol was approved by the CPP SOOM III ethics committee  
135 (number 2017-A00064-49) and complied with the Declaration of Helsinki.

### 136 **Experimental setup**

137 Participants were seated in an isokinetic dynamometer chair (Biodex System 3, Biodex  
138 Medical Systems Inc., Shirley, NY, USA). Participants' right hand was firmly strapped in a  
139 neutral position to a custom-built accessory adapted for wrist isometric contraction. The  
140 rotation axis of the dynamometer was aligned with the styloid process of the ulna. The upper  
141 arm was vertical along the trunk (shoulder abduction and elevation angles at  $0^\circ$ ), and the  
142 forearm was semipronated and flexed at  $90^\circ$ . First, participants familiarized themselves with  
143 the voluntary force production feedback procedure during an approximately 5-min warm-up  
144 of wrist flexions. Next, they received online visual feedback of the real-time exerted force  
145 contraction on a computer screen located 1 m in front of them. Then, participants performed  
146 three maximal voluntary isometric contractions lasting 3 seconds with verbal encouragement,  
147 separated by at least 30 seconds of rest in between. The maximum of the three trials was  
148 defined as the participant's maximal voluntary isometric contractions.

149 **Electromyographic recordings**

150 Surface electromyographic (EMG) activity was recorded from the right flexor carpi radialis  
151 (FCR) using two silver-chloride (Ag/AgCl) electrodes placed over the muscle belly at 1/3 of  
152 the distance from the medial epicondyle of the humerus to the radial styloid process. In  
153 addition, a ground electrode was placed over the medial epicondyle to the radial styloid.  
154 Signals were amplified (gain of 1000), band-pass filtered (10–1000 Hz), digitized at a  
155 sampling rate of 2000 Hz and stored for off-line analysis (Biopac Systems Inc. Goleta, CA,  
156 USA).

157 Background root mean square (RMS) of the surface EMG was calculated during the 100 ms  
158 epoch before TMS to ensure the absence of muscle contraction in each condition.

159 **Transcranial Magnetic Stimulation**

160 Transcranial magnetic stimuli were applied using a 70-mm figure-of-eight coil through a  
161 Magstim BiStim<sup>2</sup> stimulator (The Magstim Co., Whitland, UK) with a monophasic current  
162 waveform. The optimal stimulation site on the scalp (hotspot) was defined as the location  
163 eliciting the largest MEP amplitude in the FCR muscle with PA-induced currents for a given  
164 intensity. This location was marked by a color marker on a tight-fitting cap worn by the  
165 participant. For other coil orientations, the same hotspot was used since previous experiments  
166 have shown that the direction of the induced current does not significantly influence the  
167 position of the hotspot (Sakai *et al.*, 1997; Hamada *et al.*, 2013) (see Figure 1).

168

169 Please Insert Fig. 1 here

170

171 The resting motor threshold (rMT) was determined for PA and AP directions as the lowest  
172 stimulus intensity required to evoke at least 5 MEPs of 50  $\mu$ V peak-to-peak amplitude out of  
173 10 consecutive trials in the relaxed muscle (Rossini *et al.*, 1994). The active motor threshold  
174 (aMT) was determined for PA, LM and AP directions as the lowest stimulus intensity  
175 required to evoke at least 5 MEPs of 200  $\mu$ V peak-to-peak amplitude out of 10 consecutive  
176 trials during 10% of their Maximal Voluntary Contraction (MVC) (Rossini *et al.*, 1994).

## 177 **MEPs latency**

178 The onset latency of MEPs obtained between PA-LM and AP-LM was used as an individual  
179 index of early (I1) and late (I2, I3) I-waves recruitment (Hamada *et al.*, 2013; Neige &  
180 Beynel, 2020).

181 MEPs onset latency was determined for the FCR while participants maintained approximately  
182 10% of their MVC, with online feedback visualizing the generated force recorded by the  
183 isokinetic dynamometer (Hamada *et al.*, 2013). This was done to ensure that low stimulus  
184 intensities could be used, thereby maximizing the selectively recruiting early or late I-waves  
185 with PA or AP currents. Higher stimulus intensity was used for LM to ensure that  
186 corticospinal neurons were directly stimulated (D-wave) at this coil orientation (Werhahn *et*  
187 *al.*, 1994). Stimulation intensities were set at 110% of  $aMT_{PA}$ , 110% of  $aMT_{AP}$  and 150% of  
188  $aMT_{LM}$  (or 50% of maximum stimulator output (%MSO) in participants whose 150%  $aMT_{LM}$   
189 did not reach 50 %MSO) (Hamada *et al.*, 2013). Fifteen MEPs were recorded for each current  
190 direction, with the order of currents pseudo-randomized. The participants were instructed to  
191 maintain their contraction, and the interval between stimulations was fixed at 4s. At the end of  
192 each condition (i.e., 15 trials) participants were asked to relax their wrists to avoid fatigue.  
193 The onset latency of MEPs assessed during muscle contraction was measured from the  
194 superimposed raw EMG waves-forms by visual inspection (Hamada *et al.*, 2013; Hannah,  
195 Rocchi, *et al.*, 2018).

## 196 **Adaptive threshold-hunting technique**

197 To probe the distinct cortical elements recruited within M1 during MI, we used the adaptive  
198 threshold-hunting technique, which consists in maintaining a constant MEP amplitude (called  
199 the  $MEP_{target}$ , see below) by adjusting the TS (Test Stimulus) stimulation intensity. The  
200 adaptive threshold-hunting paradigm offers several advantages when compared to the  
201 conventional protocol used to assess corticospinal excitability and SICI modulations. First, it  
202 allows for overcoming the intrinsic MEPs amplitude variability, thus providing more reliable  
203 results with a shorter acquisition time (Samusyte *et al.*, 2018). Then, it minimizes the  
204 potential “floor/ceiling effect” when complete inhibition is observed with the conventional  
205 SICI paradigm (Cirillo & Byblow, 2016). Finally, the adaptive threshold-hunting technique  
206 relies on a weaker TS intensity (see below) than conventional paradigms (usually  $MEP_{test}$   
207 1mV or 120-130% rMT), which is thought to recruit more selectively early and later I-waves  
208 generating pathways (Di Lazzaro *et al.*, 2001; Cirillo *et al.*, 2020).



209 In the current study, unconditioned  $MEP_{test}$  and SICI modulation obtained during MI and  
210 compared to the rest will be assessed by using the adaptive threshold-hunting technique with  
211 PA and AP current orientations known to elicit early- preferentially and late I-waves,  
212 respectively.

### 213 **$MEP_{target}$**

214 The hunting threshold was defined as the TS intensity (expressed in %MSO) required to elicit  
215 a  $MEP_{target}$  in the relaxed FCR muscle corresponding to the mean of 15 MEPs elicited at  
216 115%  $rMT_{PA}$  in peak-to-peak amplitude. This led to a  $MEP_{target}$  of  $0.251 \pm 0.141$  mV  
217 amplitude (see Table 1 for individual values). Generally, a non-personalized fixed 0.2 mV  
218  $MEP_{target}$  amplitude is selected in studies using the adaptive threshold-hunting technique,  
219 corresponding approximately to 109% rMT (Fisher *et al.*, 2002; Awiszus, 2003; Vucic *et al.*,  
220 2006; Menon *et al.*, 2015; Cirillo & Byblow, 2016; Cirillo *et al.*, 2018; Samusyte *et al.*, 2018;  
221 Van den Bos *et al.*, 2018; Neige *et al.*, 2020). However, in the current study, a subject-  
222 specific  $MEP_{target}$  was chosen since 1) a huge between-subject variability in the intrinsic  
223 excitability of the corticospinal pathway exists, 2) a TS delivered at a lower intensity (i.e.,  
224 below 110% rMT) could fail to evoke late I-waves, and limits SICI magnitude (Garry &  
225 Thomson, 2009) and 3) a TS delivered at a higher intensity can also elicit early I-waves when  
226 using an AP current direction, therefore limiting the interpretation differences obtained  
227 between PA and AP findings.

### 228 **Single-pulse TMS**

229 The adaptive threshold-tracking single-pulse TMS technique was used to assess the  
230 unconditioned TS stimulation intensity required to reach the  $MEP_{target}$  amplitude (see General  
231 procedure) at rest vs. during MI, with PA and AP currents direction. The unconditioned TS  
232 intensity (expressed in %MSO) was quantified and compared across all experimental  
233 conditions.

### 234 **Short-interval intracortical inhibition (SICI)**

235 The adaptive threshold-hunting technique was then used to investigate SICI modulation at rest  
236 vs. during MI, with PA and AP currents direction. A sub-threshold conditioning pulse (CS)  
237 was applied before the TS. The conditioned TS stimulation intensity required to reach the  
238  $MEP_{target}$  amplitude was quantified. The CS intensity was fixed at 60%  $rMT_{PA}$  for  $SICI_{PA}$  and  
239 60%  $rMT_{AP}$  for  $SICI_{AP}$ , based on a previous study showing that higher CS intensities could

240 lead to the unwanted recruitment of excitatory interneurons during MI, biasing the result  
241 interpretation (Neige *et al.*, 2020). The inter-stimulus interval (ISI) between CS and TS was  
242 set at 3 ms to induce the greatest inhibition when using the AP current direction (Kujirai *et*  
243 *al.*, 1993; Cirillo *et al.*, 2018).

244 To probe the influence of the Task and Orientation on intracortical inhibition, the amount of  
245 SICI (expressed in INH%) was quantified for each condition using the following equation  
246 (Fisher *et al.*, 2002):

$$INH(\%) = \frac{(\text{conditioned TS Intensity}) - (\text{unconditioned TS Intensity})}{(\text{unconditioned TS Intensity})} \times 100$$

247 The higher values characterize the higher TS Intensity required to overcome the inhibitory  
248 influence of the CS and reach the MEP<sub>target</sub> amplitude (Cirillo *et al.*, 2020).

249 It has to be noted that only SICI data from 15 participants were used in the subsequent  
250 analysis because it was not possible to reach the MEP<sub>target</sub> amplitude even at high stimulation  
251 intensity (>90% MSO) in 2 participants.

## 252 **General procedure**

253 Experimental conditions (single- vs. paired-pulse; rest vs. MI; PA vs. AP current direction)  
254 were performed in different recording blocks and were randomized and counterbalanced  
255 across participants. An available online freeware (TMS Motor Threshold Assessment Tool,  
256 MTAT 2.0), based on a maximum-likelihood Parameter Estimation by Sequential Testing  
257 (PEST) strategy (Awiszus, 2003) was used with “assessment without a priori information” in  
258 line with previous studies (Cirillo & Byblow, 2016; Cirillo *et al.*, 2018). The stimulation  
259 sequence always began with the TS at 37 %MSO. One experimenter held the coil over M1,  
260 while the other indicated whether (or not) the MEP amplitude was  $\geq$  MEP<sub>target</sub>. The predictive  
261 algorithm then determined the next TS intensity to be delivered and was stopped after twenty  
262 stimulations, which provides sufficient accuracy for the threshold estimate according to  
263 previous studies (Awiszus, 2003, 2014; Ah Sen *et al.*, 2017).

264 For MI trials, participants were instructed to perform explicit and kinesthetic (somatosensory)  
265 MI of right wrist maximal isometric contractions with the first-person perspective for a  
266 duration of 3 s following an auditory cue (Hanakawa, 2016). Participants were reminded that  
267 they had already performed this movement during maximal contractions at the beginning of  
268 the experiment. The following instructions (in French) were carefully given to the

269 participants: “When you hear the cue, try to imagine yourself performing the movement,  
270 feeling the movement, i.e., the muscle contraction and the tension that you would experience  
271 when performing the actual action. Be sure not to contract any muscles during the task and  
272 keep your eyes open” (Lebon *et al.*, 2019; Neige *et al.*, 2021). The kinesthetic MI strategy is  
273 thought to produce the greater muscle-specific and temporally modulated facilitation of the  
274 corticospinal pathway compared to the visual MI strategy (Stinear *et al.*, 2006). The TMS  
275 pulses were triggered  $1250 \pm 250$  ms after the onset of the auditory cue during the execution  
276 phase of MI trials (Neige *et al.*, 2021) and the inter-trial interval was 8 s. Finally, the RMS  
277 preceding the TS for each trial was inspected during the experiment. Trials contaminated by  
278 pre-stimulus EMG activity (RMS  $>10 \mu\text{V}$ ; 100 ms before stimulation) were rejected online  
279 and repeated immediately (Mooney *et al.*, 2018).

## 280 **Statistical analysis**

281 Statistical analyses were performed using Statistical Program for the Social Sciences (SPSS)  
282 version 24 software (SPSS Inc., Chicago, IL, USA). Data distribution was assessed using the  
283 Shapiro-Wilk test. Homogeneity of variances was assessed by Mauchly’s test. If the  
284 sphericity assumption was violated, a Greenhouse-Geiser correction was applied. Pre-planned  
285 posthoc analyses were performed on significant interactions after applying a Bonferroni  
286 adjustment for multiple comparisons. Corrected p values for multiple comparisons are  
287 reported in the results section. The  $\alpha$  level for all analyses was fixed at .05. Partial eta squared  
288 ( $\eta_p^2$ ) values are reported to express the portion of the total variance attributable to the tested  
289 factor or interaction. For t-test analyses, effect sizes (Cohen’s d) are reported to indicate small  
290 ( $d = 0.2$ ), moderate ( $d = 0.5$ ) and large ( $d = 0.8$ ) comparative effects. Values in parentheses in  
291 the text represent mean  $\pm$  SD.

292 The first set of analyses was performed to control for potential methodological biases. A  
293 Student’s two-tailed paired sample *t*-tests were used to compare the rMT and aMT (%MSO)  
294 obtained for PA and AP current direction and to analyze the MEPs latency difference between  
295 PA-LM and AP-LM.

296 Then, a repeated-measure ANOVA was performed on the unconditioned TS Intensity  
297 (%MSO) with two within-subject factors: Task<sub>2</sub> (Rest vs. MI) and Orientation<sub>2</sub> (PA vs. AP).  
298 Moreover, to complement this analysis and test specifically how changes observed between  
299 rest and MI differ according to the Orientation, MI-rest ratios were calculated and compared  
300 (PA vs. AP) by using a two-tailed Student *t*-test for paired samples.

301 The same repeated-measure ANOVA was also performed on SICI measurements (INH %)   
302 with Task<sub>2</sub> (Rest vs. MI) and Orientation<sub>2</sub> (PA vs. AP) within-subject factors.

303 The RMS values were compared across conditions using a repeated-measures analysis of   
304 variance (ANOVA) with two within-subject factors: Task<sub>2</sub> (Rest vs. MI), and Orientation<sub>2</sub>   
305 (PA vs. AP). This ANOVA was performed separately for the unconditioned TS and the SICI   
306 measures. We predict no significant difference for these comparisons since an absence of any   
307 volitional muscle activity is expected for all the experimental conditions.

## 308 **Results**

### 309 **Motor thresholds**

310 Overall, both rMT ( $t(16) = -3.55$ ,  $p = .003$ ; Cohen's  $d = -0.862$ ) and aMT ( $t(16) = -8.147$ ,  $p$    
311  $< .001$ ; Cohen's  $d = -1.976$ ) were significantly lower for PA compared to AP orientation   
312 (Table 1) as observed in previous studies using the adaptive-hunting threshold technique   
313 (Cirillo & Byblow, 2016; Cirillo *et al.*, 2018).

314

315 Please Insert Table 1 here

316

### 317 **MEP latency**

318 The analysis of MEPs latency difference revealed that PA-LM latency was significantly   
319 shorter compared with AP-LM latency ( $0.90 \pm 0.7$  ms vs.  $2.56 \pm 1.1$  ms;  $t(16) = -10.042$ ,  $p <$    
320  $.001$ ; Cohen's  $d = -2.436$ ). This result was consistent across participants and suggested that   
321 the early wave recruited with PA orientation (mean latency =  $17.06 \pm 1.2$  ms) and late I-   
322 waves recruited with AP orientation (mean latency =  $18.72 \pm 1.4$  ms) could be differentially   
323 recruited within individuals.

### 324 **Unconditioned TS Intensity**

325 Figure 3A illustrates the unconditioned TS Intensity obtained at rest and during MI for PA   
326 and AP current directions. We found a significant main effect of Orientation ( $F_{(1,16)} = 39.338$ ,   
327  $p < .001$ ;  $\eta_p^2 = .711$ ) indicating that the unconditioned TS Intensity required to reach the   
328 MEP<sub>target</sub> was significantly higher for the AP orientation than the PA orientation. A main   
329 effect of Task was also observed ( $F_{(1,16)} = 11.004$ ,  $p = .004$ ;  $\eta_p^2 = .409$ ) but more importantly

330 the Orientation by Task interaction was significant ( $F_{(1,16)} = 5.130$ ,  $p = .038$ ;  $\eta_p^2 = .243$ ). Post  
331 hoc analyses revealed that for both PA and AP orientations, the unconditioned TS Intensity  
332 required to reach the  $MEP_{target}$  was significantly lower during MI than at rest ( $p = .005$  for PA  
333 and  $p = .025$  for AP) indicating that MI increased corticospinal excitability. Importantly, when  
334 comparing the rest vs. MI ratios according to the Orientation, the reduction of the  
335 unconditioned TS Intensity for MI when compared to rest was significantly more important  
336 for PA than AP direction ( $t(16) = -2.601$ ,  $p = .019$ ; Cohen's  $d = -0.631$ ) (see Figure 3B).  
337  
338 Taken together, these results suggest that the classical corticospinal excitability increase  
339 during MI is mainly driven by early I-waves recruitment.

340

341

Please Insert Fig. 2 here

342

### 343 **Conditioned TS Intensity (SICI)**

344 Figure 4 illustrates the percentage of inhibition (SICI) obtained at rest and during MI for the  
345 PA and AP current direction. We did not find any main effects of Orientation ( $F_{(1,14)} = 1.107$ ,  
346  $p = .311$ ) or Task ( $F_{(1,14)} < 1$ ,  $p = .895$ ), but the Orientation by Task interaction was significant  
347 ( $F_{(1,14)} = 11.995$ ,  $p = 0.004$ ,  $\eta_p^2 = .461$ ). Post hoc comparisons showed that at rest, the amount  
348 of SICI was higher for AP orientation than the PA orientation ( $p = .031$ ) whereas it was not  
349 significant when comparing orientations during MI ( $p = .106$ ). Moreover, SICI was greater  
350 during MI compared to rest with the PA orientation ( $p = .028$ ), whereas SICI was lower  
351 during MI compared to rest with the AP orientation ( $p = .033$ ).

352

353

Please Insert Fig. 3 here

354

### 355 **RMS**

356 The analysis of RMS of EMG background for the unconditioned TS showed no significant  
357 difference between PA and AP orientation ( $F_{(1,16)} < 1$ ,  $p = .548$ ) and more importantly  
358 between rest and MI ( $F_{(1,16)} < 1$ ,  $p = .542$ ). Nor was the Orientation by task interaction ( $F_{(1,16)}$   
359  $= 3.594$ ,  $p = .076$ ).

360 Similarly, the analysis of the RMS values for the conditioned TS yielded no significant main  
361 effect of Orientation ( $F_{(1,14)} < 1$ ,  $p = .997$ ), Task ( $F_{(1,14)} = 1.77$ ,  $p = .204$ ) or Orientation by  
362 Task Interaction ( $F_{(1,13)} < 1$ ,  $p = .563$ ).

363 Together, these results indicate that any changes in corticospinal excitability cannot be  
364 attributed to differences in the EMG levels prior to the TMS pulse.

## 365 **Discussion**

366 In the current study, we demonstrated for the first time that MI activates different subsets of  
367 neurons within M1 by means of directional TMS and the adaptive threshold-hunting  
368 technique. The increase of corticospinal excitability during MI may originate from an increase  
369 in the excitability of the pathway known to generate early I-waves rather than the pathway  
370 that preferentially generates late I-waves, as evidenced by a greater increase observed with  
371 PA orientation when compared to AP orientation. By using paired-pulse stimulation, the  
372 results confirmed that the amount of SICI measured at rest is higher for AP orientation than  
373 the PA orientation (Neige *et al.*, 2020). Interestingly, the SICI increase observed during MI  
374 (vs. at rest) was also restricted to PA orientation. On the contrary, when using AP orientation  
375 SICI was lower during MI compared to rest. Taken together, it suggests that pathways  
376 recruited by PA and AP orientations generating early- and late I-waves respectively are  
377 differentially modulated by MI. This result also confirms the hypothesis that MI activates  
378 neural circuits downstream of the pyramidal cells and produces a subliminal motor output that  
379 reaches the spinal level (Grosprêtre *et al.*, 2015) rather than induces a specific superficial  
380 activation restricted to the superficial layers within M1 that could explain the absence of  
381 muscle activity during motor imagery (Persichetti *et al.*, 2020). The excitability of the  
382 pathway activated by PA orientation that generates early I-wave may be critical in modulating  
383 both corticospinal excitability and intracortical inhibition.

## 384 **Corticospinal excitability increase observed during MI is greater for PA than AP** 385 **orientation**

386 It is well known that MEPs amplitude increases during MI compared to rest reflect an  
387 increase in neuron responsiveness to TMS (Grosprêtre *et al.*, 2016). However, MI is a  
388 complex state that also involves mechanisms that actively suppress the transmission of the  
389 motor command into the efferent pathway, supporting the action of inhibitory pathways  
390 during MI (Jeannerod & Decety, 1995). Actually, it is still unclear which inhibitory

391 mechanisms counteract the corticospinal excitability increase in order to prevent the  
392 production of an overt movement.

393 Based on previous reports demonstrated that single-pulse TMS with a PA orientation  
394 preferentially recruits early I-waves (I1), whereas AP orientation preferentially recruits later I-  
395 waves (I3) (Zoghi *et al.*, 2003; Di Lazzaro *et al.*, 2017), we used directional TMS to activate  
396 different sets of excitatory synaptic inputs within M1.

397 First, our results demonstrate that our experimental setting (coil orientation) was correct, with  
398 a significant latency difference between PA-LM and AP-LM, supporting differential  
399 recruitment of cortical neurons in M1 relative to the current orientation (Werhahn *et al.*, 1994;  
400 Hamada *et al.*, 2013; Di Lazzaro & Rothwell, 2014). If it has already been shown in a forearm  
401 extensor muscle (McCambridge *et al.*, 2015), our study is the first to demonstrate latency  
402 difference in the FCR muscle.

403 To further investigate the involvement of different subsets of cortical neurons during MI  
404 compared to the resting state, we used the adaptive threshold-hunting technique and compared  
405 the unconditioned TS intensity (%MSO) required to reach the  $MEP_{target}$  at rest and during MI  
406 with PA and AP orientation. We found that the unconditioned TS Intensity required to reach  
407 the  $MEP_{target}$  was significantly lower during MI than at rest for both the PA and the AP  
408 orientations. However, when comparing the ratios MI/rest according to the orientation, the  
409 reduction of the unconditioned TS Intensity for MI was significantly more important for PA  
410 than AP direction. Taken together, these results indicate that the early I-wave generating  
411 pathway within M1 possibly mediated the MEPs amplitude increases observed during MI.  
412 The exact underpinning neurophysiology of I-waves generation remains largely  
413 misunderstood (Ziemann, 2020). However, it has been suggested that the early I-wave evoked  
414 by TMS with PA orientation is the result of the activation of monosynaptic cortico-cortical  
415 connections projecting onto the large corticospinal neurons of layer V (Di Lazzaro &  
416 Ziemann, 2013; Di Lazzaro *et al.*, 2017; Hannah, 2020). This result seems coherent with  
417 previous literature assuming that the early I-wave is produced by a different anatomical  
418 substrate and mechanism than the late I-waves (Ziemann, 2020). Crucially, specific early I-  
419 wave recruitment evoked by TMS with PA orientation is enhanced when corticospinal  
420 excitability increases (Di Lazzaro *et al.*, 1998a, 2017), which was the case during MI. For  
421 example, voluntary muscle contraction increased both corticospinal excitability and the  
422 relative contribution of the early I-wave (Di Lazzaro *et al.*, 1998a, 2017).

423 The findings of the current study also extend and consolidate our knowledge regarding the

424 distinct I-wave circuits recruitment during behavioral states that share analogous control  
425 mechanisms and neural circuits with overt movements but without any muscle activity (i.e.,  
426 covert actions) (Hannah, 2020). Indeed, recent studies exploited the directional TMS  
427 technique to probe the different subsets of cortical neurons recruited during motor preparation  
428 (Hannah, Cavanagh, *et al.*, 2018) and action observation (Hannah, Rocchi, *et al.*, 2018). The  
429 results showed that during motor preparation, the decrease of the corticospinal excitability in  
430 the selected and non-selected muscles was accompanied by selective suppression of the subset  
431 of excitatory inputs to corticospinal neurons responsible for late I-waves. In contrast, the  
432 subsets of neurons responsible for early-I wave generation remain unaffected (Derosiere,  
433 2018; Hannah, Cavanagh, *et al.*, 2018). However, when using the directional TMS technique  
434 during action observation, other authors failed to observe selective recruitment of the early or  
435 late I-waves pathway, probably due to large intersubject variability in corticospinal  
436 modulations (Hannah, Rocchi, *et al.*, 2018). Overall, the recent use of the directional TMS  
437 technique applied during motor preparation, action observation and MI allows further insight  
438 into the distinct circuitry recruited with TMS that contributes to the corticospinal excitability  
439 modulation.

#### 440 **SICI increase during MI is restricted to PA orientation**

441 The adaptive threshold-hunting paired-pulse TMS technique was also used in the current  
442 study to examine modulations of SICI during MI and at rest and how they are influenced by  
443 TMS coil orientation.

444 SICI involves a subthreshold CS, which is thought to activate low-threshold inhibitory  
445 interneurons that employ gamma-aminobutyric acid type A receptor (GABA<sub>A</sub>). The effect of  
446 the activation of these GABAergic inhibitory interneurons is the reduction of the excitatory  
447 inputs activated by the TS (Kujirai *et al.*, 1993; Di Lazzaro *et al.*, 1998b, 2017). Importantly,  
448 it has been described previously that SICI affects predominantly later I-waves (I<sub>3</sub>), mainly  
449 targeted by AP orientations (Nakamura *et al.*, 1997; Hanajima *et al.*, 1998; Di Lazzaro *et al.*,  
450 2012; Higashihara *et al.*, 2020). Moreover, it is known that the use of the adaptive threshold-  
451 tracking technique with an AP-induced current with a 3-ms ISI provides a more robust and  
452 sensitive measure of SICI than with a PA-induced current (Cirillo & Byblow, 2016).  
453 Therefore, a greater level of SICI assessed at rest using AP- compared with PA-orientation  
454 demonstrated in the present study corroborates and replicates earlier findings (Cirillo &  
455 Byblow, 2016; Cirillo *et al.*, 2018, 2020). This result also indicates further evidence that SICI



456 is mediated by the recruitment of inhibitory interneurons generating late I-waves.  
457 By comparing the extent of SICI modulation obtained with a PA-induced current, we found  
458 that there was significantly more inhibition during MI when compared to rest. This finding  
459 also corroborates a previous study showing that when tested with low CS intensities, as in the  
460 current study ( $< 70\%$  rMT), SICI is greater during MI than at rest (Neige *et al.*, 2020). This  
461 increase in SICI could reflect the crucial role played by cortical interneurons within M1 in the  
462 fine-tuning neural processes required during MI. This may prevent the production of an overt  
463 movement when the mental representation of that movement is activated.  
464 Conversely, by comparing the extent of SICI modulation obtained with an AP-induced  
465 current, we found a SICI decrease during MI compared to rest. Moreover, contrary to what  
466 was found during the resting state, the level of SICI assessed during MI using AP- compared  
467 with PA orientation was not significantly greater. These results, combined with the  
468 unconditioned TS intensity findings, indicate that the specific early- and late I-waves evoked  
469 by PA and AP orientation are differentially modulated by MI.

#### 470 **MI influences a specific distributed circuit that can differentially contribute to early and** 471 **late I-waves**

472 Neuroimaging studies provided evidence that MI activates a premotor-parietal network,  
473 including cortical and subcortical brain regions such as the dorsolateral prefrontal cortex,  
474 supplementary motor area, premotor cortex, posterior parietal regions, putamen and  
475 cerebellum (Hardwick *et al.* 2018). Crucially, M1 is known to integrate inputs from some of  
476 these structures, and the latter are differentially recruited according to the current orientation.  
477 For example, late I-waves evoked by AP orientation could activate axons of neurons of the  
478 premotor cortex projecting to the corticospinal cells (Groppa *et al.*, 2012; Volz *et al.*, 2015;  
479 Aberra *et al.*, 2020; Siebner, 2020; Desmons *et al.*, 2021). Recently, Oldrati *et al.* (2021)  
480 reported that following offline 1Hz inhibitory repetitive TMS over the dorsal premotor cortex  
481 (PMd), corticospinal excitability assessed during kinesthetic MI was not significantly higher  
482 than rest condition (Oldrati *et al.*, 2021). These findings suggest facilitatory connectivity from  
483 PMd to M1 during MI. Although this remains speculative, the facilitatory input from PMd to  
484 M1 during MI has decreased the SICI level within M1. Moreover, the opposite higher level of  
485 SICI during MI (vs. rest) observed with PA current reflect the activation of inhibitory inputs  
486 received from the somatosensory cortex and the supplementary motor area, both areas known  
487 to functionally inhibit M1 when imagining (Kasess *et al.*, 2008; Oldrati *et al.*, 2021). Finally,

488 it is also possible that the cerebellum, which facilitates M1 excitability during MI (Tanaka *et*  
489 *al.*, 2018; Rannaud Monany *et al.*, 2022), also contributes to the result of the current study  
490 since the influence of the cerebellum on M1 might occur via interactions with specific I-  
491 waves generating circuits (Spampinato *et al.*, 2020).

## 492 **Limitations and perspectives**

493 Several limitations need to be taken into consideration when interpreting the results of this  
494 study. First, SICI modulations tested with the adaptive-threshold hunting technique also  
495 depend on CS intensity (particularly during MI) (Vucic *et al.*, 2009; Ibáñez *et al.*, 2020; Neige  
496 *et al.*, 2020) and interstimulus intervals (Fisher *et al.*, 2002). These two parameters were not  
497 manipulated in the current study, and the careful consideration of stimulation parameters  
498 selected for SICI assessment deserves further investigations. Moreover, the activation of  
499 distinct subsets of neurons within M1 according to the PA or AP orientation is known to be  
500 sensitive to specific stimulation parameters such as pulse duration, pulse shape, and phase-  
501 amplitude (D'Ostilio *et al.*, 2016; Hannah & Rothwell, 2017; Hannah *et al.*, 2020;  
502 Spampinato, 2020).

503 Future studies should use a controllable pulse parameter TMS device with 1) monophasic  
504 pulses and 2) short duration pulses (i.e., 30  $\mu$ s) for AP current and long duration pulses (i.e.  
505 120  $\mu$ s) for PA current to determine whether the different activation of subsets of neurons in  
506 AP and PA current change during MI.

507 To gain further insight into the different subsets of cortical neurons and interneuronal circuits  
508 recruited during MI, it would be worthwhile to exploit recent techniques also developed to  
509 probe the separate subsets of inputs within M1. For example, Kurz *et al.* (2019) developed a  
510 novel non-invasive method that combines single-pulse TMS with peripheral nerve  
511 stimulations of the median nerve generating an H-reflex. This technique makes it possible to  
512 estimate excitability changes of different micro-circuits of M1, which reflect layer-specific  
513 activity (Dukkipati & Trevarrow, 2019; Kurz *et al.*, 2019). Since layer-specific cortical  
514 circuits activity has been recently evidenced during MI (Persichetti *et al.*, 2020) and  
515 corticospinal neurons responsible for the early and late I-waves pathways are thought to  
516 originate from layer-specific cortical circuits, the technique of Kurz *et al.* could be a  
517 promising tool to delineate further the different subsets of neurons in M1 activated during MI.  
518 Finally, the exact contribution of the early and late I-waves can be captured by delivering  
519 paired-pulse TMS at precise intervals approximating the different I-wave latency (Tokimura

520 *et al.*, 1996; Hanajima *et al.*, 2002). This technique has been recently applied during grasping  
521 observation to isolate the contribution to early and late excitatory inputs to M1 (Cretu *et al.*,  
522 2020) and could be tested during MI.

523 In conclusion, this study is the first to present evidence that the increase of corticospinal  
524 excitability and intracortical inhibition during MI may originate from a specific modulation of  
525 the excitability of the pathway activated by PA orientation that generates early I-wave (rather  
526 than later I-waves generated by AP orientation). This finding is reflected by a greater  
527 corticospinal excitability increase observed during MI (compared to rest) with PA than AP  
528 orientation. Moreover, the SICI increase during MI was only restricted to PA orientation. We  
529 found decreased SICI when using AP orientation, which is more sensitive to later I-waves  
530 generating pathways. Taken together, the results confirm that MI modulates the excitability of  
531 the pathway that generates early I-wave preferentially.

### 532 **Competing interests**

533 The authors declare no competing interests.

534 **References**

- 535 Aberra, A.S., Wang, B., Grill, W.M., & Peterchev, A.V. (2020) Simulation of transcranial  
536 magnetic stimulation in head model with morphologically-realistic cortical neurons. *Brain*  
537 *Stimulation*, **13**, 175–189.
- 538 Ah Sen, C.B., Fassett, H.J., El-Sayes, J., Turco, C. V., Hameer, M.M., & Nelson, A.J. (2017)  
539 Active and resting motor threshold are efficiently obtained with adaptive threshold hunting.  
540 *PLoS ONE*, **12**, 1–9.
- 541 Anderson, C.T., Sheets, P.L., Kiritani, T., & Shepherd, G.M.G. (2010) Sublayer-specific  
542 microcircuits of corticospinal and corticostriatal neurons in motor cortex. *Nature*  
543 *neuroscience*, **13**, 739–744.
- 544 Awiszus, F. (2003) TMS and threshold hunting. *Supplements to Clinical neurophysiology*, **56**,  
545 13–23.
- 546 Awiszus, F. (2014) Using relative frequency estimation of transcranial magnetic stimulation  
547 motor threshold does not allow to draw any conclusions about true threshold. *Clinical*  
548 *Neurophysiology*, **125**, 1285–1286.
- 549 Cirillo, J. & Byblow, W.D. (2016) Threshold tracking primary motor cortex inhibition: The  
550 influence of current direction. *European Journal of Neuroscience*, **44**, 2614–2621.
- 551 Cirillo, J., Semmler, J.G., Mooney, R.A., & Byblow, W.D. (2018) Conventional or threshold-  
552 hunting TMS? A tale of two SICIs. *Brain stimulation*, **11**, 1296–1305.
- 553 Cirillo, J., Semmler, J.G., Mooney, R.A., & Byblow, W.D. (2020) Primary motor cortex  
554 function and motor skill acquisition: insights from threshold-hunting TMS. *Experimental*  
555 *brain research*,.
- 556 Cretu, A.L., Ruddy, K.L., Post, A., & Wenderoth, N. (2020) Muscle-specific modulation of  
557 indirect inputs to primary motor cortex during action observation. *Experimental Brain*  
558 *Research*, **1**.
- 559 Decety, J. (1996) The neurophysiological basis of motor imagery. *Behavioural brain*  
560 *research*, **77**, 45–52.
- 561 Derosiere, G. (2018) A Dynamical System Framework for Theorizing Preparatory Inhibition.  
562 *The Journal of Neuroscience*, **38**, 3391–3393.
- 563 Desmons, M., Rohel, A., Desgagnés, A., Mercier, C., & Massé-Alarie, H. (2021) Influence of

564 different transcranial magnetic stimulation current directions on the corticomotor control of  
565 lumbar erector spinae muscles during a static task. *Journal of Neurophysiology*, **126**, 1276–  
566 1288.

567 Di Lazzaro, V., Oliviero, A., Saturno, E., Pilato, F., Insola, A., Mazzone, P., Profice, P.,  
568 Tonali, P., & Rothwell, J. (2001) The effect on corticospinal volleys of reversing the direction  
569 of current induced in the motor cortex by transcranial magnetic stimulation. *Experimental*  
570 *Brain Research*, **138**, 268–273.

571 Di Lazzaro, V., Profice, P., Ranieri, F., Capone, F., Dileone, M., Oliviero, A., & Pilato, F.  
572 (2012) I-wave origin and modulation. *Brain Stimulation*, **5**, 512–525.

573 Di Lazzaro, V., Restuccia, D., Oliviero, A., Profice, P., Ferrara, L., Insola, A., Mazzone, P.,  
574 Tonali, P., & Rothwell, J.C. (1998a) Effects of voluntary contraction on descending volleys  
575 evoked by transcranial stimulation in conscious humans. *Journal of Physiology*, **508**, 625–  
576 633.

577 Di Lazzaro, V., Restuccia, D., Oliviero, A., Profice, P., Ferrara, L., Insola, A., Mazzone, P.,  
578 Tonali, P., & Rothwell, J.C. (1998b) Magnetic transcranial stimulation at intensities below  
579 active motor threshold activates intracortical inhibitory circuits. *Experimental brain research*,  
580 **119**, 265–268.

581 Di Lazzaro, V., Rothwell, J., & Capogna, M. (2017) Noninvasive stimulation of the human  
582 brain: Activation of multiple cortical circuits. *The Neuroscientist*, 107385841771766.

583 Di Lazzaro, V. & Rothwell, J.C. (2014) Corticospinal activity evoked and modulated by non-  
584 invasive stimulation of the intact human motor cortex. *Journal of Physiology*, **592**, 4115–  
585 4128.

586 Di Lazzaro, V. & Ziemann, U. (2013) The contribution of transcranial magnetic stimulation  
587 in the functional evaluation of microcircuits in human motor cortex. *Frontiers in neural*  
588 *circuits*, **7**, 18.

589 D’Ostilio, K., Goetz, S.M., Hannah, R., Ciocca, M., Chieffo, R., Chen, J.C.A., Peterchev, A.  
590 V., & Rothwell, J.C. (2016) Effect of coil orientation on strength-duration time constant and  
591 I-wave activation with controllable pulse parameter transcranial magnetic stimulation.  
592 *Clinical Neurophysiology*, **127**, 675–683.

593 Dukkupati, S.S. & Trevarrow, M.P. (2019) Breaking down the human motor cortex: the layer-  
594 specific measurement of corticospinal neuronal activity. *Journal of Physiology*, **597**, 4437–

595 4438.

596 Fisher, R.J., Nakamura, Y., Bestmann, S., Rothwell, J.C., & Bostock, H. (2002) Two phases  
597 of intracortical inhibition revealed by transcranial magnetic threshold tracking. *Experimental*  
598 *brain research*, **143**, 240–248.

599 Garry, M.I. & Thomson, R.H.S. (2009) The effect of test TMS intensity on short-interval  
600 intracortical inhibition in different excitability states. *Experimental Brain Research*, **193**,  
601 267–274.

602 Groppa, S., Schlaak, B.H., Münchau, A., Werner-Petroll, N., Dünneberger, J., Bäumer, T., van  
603 Nuenen, B.F.L., & Siebner, H.R. (2012) The human dorsal premotor cortex facilitates the  
604 excitability of ipsilateral primary motor cortex via a short latency cortico-cortical route. *Hum.*  
605 *Brain Mapp.*, **33**, 419–430.

606 Grosprêtre, S., Lebon, F., Papaxanthis, C., & Martin, A. (2015) New evidence of corticospinal  
607 network modulation induced by motor imagery. *Journal of Neurophysiology*, **115**, 1279–  
608 1288.

609 Grosprêtre, S., Ruffino, C., & Lebon, F. (2016) Motor imagery and cortico-spinal excitability:  
610 A review. *European Journal of Sport Science*, **16**, 317–324.

611 Hamada, M., Murase, N., Hasan, A., Balaratnam, M., & Rothwell, J.C. (2013a) The role of  
612 interneuron networks in driving human motor cortical plasticity. *Cerebral Cortex*, **23**, 1593–  
613 1605.

614 Hamada, M., Murase, N., Hasan, A., Balaratnam, M., & Rothwell, J.C. (2013b) The role of  
615 interneuron networks in driving human motor cortical plasticity. *Cerebral Cortex*, **23**, 1593–  
616 1605.

617 Hanajima, R., Ugawa, Y., Terao, Y., Enomoto, H., Shio, Y., Mochizuki, H., Furubayashi, T.,  
618 Uesugi, H., Iwata, N.K., & Kanazawa, I. (2002) Mechanisms of intracortical I-wave  
619 facilitation elicited with paired-pulse magnetic stimulation in humans. *Journal of Physiology*,  
620 **538**, 253–261.

621 Hanajima, R., Ugawa, Y., Terao, Y., Sakai, K., Furubayashi, T., Machii, K., & Kanazawa, I.  
622 (1998) Paired-pulse magnetic stimulation of the human motor cortex: Differences among I  
623 waves. *Journal of Physiology*, **509**, 607–618.

624 Hanakawa, T. (2016) Organizing motor imageries. *Neuroscience Research*, **104**, 56–63.

625 Hannah, R. (2020) Transcranial magnetic stimulation: a non-invasive window into the  
626 excitatory circuits involved in human motor behavior. *Experimental Brain Research*,.

627 Hannah, R., Cavanagh, S.E., Tremblay, S., Simeoni, S., & Rothwell, J.C. (2018) Selective  
628 Suppression of Local Interneuron Circuits in Human Motor Cortex Contributes to Movement  
629 Preparation. *The Journal of neuroscience : the official journal of the Society for*  
630 *Neuroscience*, **38**, 1264–1276.

631 Hannah, R., Rocchi, L., & Rothwell, J.C. (2018) Observing without acting: A balance of  
632 excitation and suppression in the human corticospinal pathway? *Frontiers in Neuroscience*,  
633 **12**, 1–10.

634 Hannah, R., Rocchi, L., Tremblay, S., Wilson, E., & Rothwell, J.C. (2020) Pulse width biases  
635 the balance of excitation and inhibition recruited by transcranial magnetic stimulation. *Brain*  
636 *Stimulation*, **13**, 536–538.

637 Hannah, R. & Rothwell, J.C. (2017) Pulse Duration as Well as Current Direction Determines  
638 the Specificity of Transcranial Magnetic Stimulation of Motor Cortex during Contraction.  
639 *Brain Stimulation*, **10**, 106–115.

640 Higashihara, M., Van den Bos, M.A.J., Menon, P., Kiernan, M.C., & Vucic, S. (2020)  
641 Interneuronal networks mediate cortical inhibition and facilitation. *Clinical Neurophysiology*,  
642 **131**, 1000–1010.

643 Huber, L., Handwerker, D.A., Jangraw, D.C., Chen, G., Hall, A., Stüber, C., Gonzalez-  
644 Castillo, J., Ivanov, D., Marrett, S., Guidi, M., Goense, J., Poser, B.A., & Bandettini, P.A.  
645 (2017) High-Resolution CBV-fMRI Allows Mapping of Laminar Activity and Connectivity  
646 of Cortical Input and Output in Human M1. *Neuron*, **96**, 1253-1263.e7.

647 Ibáñez, J., Spampinato, D.A., Paraneetharan, V., & Rothwell, J.C. (2020) SICI during  
648 changing brain states: Differences in methodology can lead to different conclusions. *Brain*  
649 *Stimulation*, **13**, 353–356.

650 Jeannerod, M. & Decety, J. (1995) Mental motor imagery: a window into the representational  
651 stages of action. *Current Opinion in Neurobiology*, **5**, 727–732.

652 Kasess, C.H., Windischberger, C., Cunnington, R., Lanzenberger, R., Pezawas, L., & Moser,  
653 E. (2008) The suppressive influence of SMA on M1 in motor imagery revealed by fMRI and  
654 dynamic causal modeling. *NeuroImage*, **40**, 828–837.

655 Kujirai, T., Caramia, M.D., Rothwell, J.C., Day, B.L., Thompson, P.D., Ferbert, A., Wroe, S.,

656 Asselman, P., & Marsden, C.D. (1993) Corticocortical inhibition in human motor cortex. *The*  
657 *Journal of Physiology*, **471**, 501–519.

658 Kurz, A., Xu, W., Wiegel, P., Leukel, C., & N. Baker, S. (2019) Non- invasive assessment of  
659 superficial and deep layer circuits in human motor cortex. *The Journal of Physiology*, **597**,  
660 2975–2991.

661 Lebon, F., Byblow, W.D., Collet, C., Guillot, A., & Stinear, C.M. (2012) The modulation of  
662 motor cortex excitability during motor imagery depends on imagery quality. *European*  
663 *Journal of Neuroscience*, **35**, 323–331.

664 Lebon, F., Ruffino, C., Greenhouse, I., Labruna, L., Ivry, R.B., & Papaxanthis, C. (2019) The  
665 Neural Specificity of Movement Preparation During Actual and Imagined Movements.  
666 *Cerebral Cortex*, **29**, 689–700.

667 Li, S., Latash, M.L., & Zatsiorsky, V.M. (2004) Effects of motor imagery on finger force  
668 responses to transcranial magnetic stimulation. *Cognitive Brain Research*, **20**, 273–280.

669 McCambridge, A.B., Stinear, J.W., & Byblow, W.D. (2015) “I-wave” recruitment determines  
670 response to tDCS in the Upper Limb, but only so Far. *Brain Stimulation*, **8**, 1124–1129.

671 Menon, P., Geevasinga, N., Yiannikas, C., Howells, J., Kiernan, M.C., & Vucic, S. (2015)  
672 Sensitivity and specificity of threshold tracking transcranial magnetic stimulation for  
673 diagnosis of amyotrophic lateral sclerosis: A prospective study. *The Lancet Neurology*, **14**,  
674 478–484.

675 Mooney, R.A., Cirillo, J., & Byblow, W.D. (2018) Adaptive threshold hunting reveals  
676 differences in interhemispheric inhibition between young and older adults. *The European*  
677 *journal of neuroscience*, **48**, 2247–2258.

678 Nakamura, H., Kitagawa, H., Kawaguchi, Y., & Tsuji, H. (1997) Intracortical facilitation and  
679 inhibition after transcranial magnetic stimulation in conscious humans. *Journal of Physiology*,  
680 **498**, 817–823.

681 Neige, C. & Beynel, L. (2020) New insight on the role of late indirect- wave pathway  
682 underlying theta- burst stimulation- induced plasticity. *The Journal of Physiology*, **598**, 217–  
683 219.

684 Neige, C., Lebon, F., Mercier, C., Gaveau, J., Papaxanthis, C., & Ruffino, C. (2021) Pain, No  
685 Gain: Acute Pain Interrupts Motor Imagery Processes and Affects Mental Training-Induced  
686 Plasticity. *Cerebral Cortex*, 1–12.



687 Neige, C., Rannaud Monany, D., Stinear, C.M., Byblow, W.D., Papaxanthis, C., & Lebon, F.  
688 (2020) Unravelling the Modulation of Intracortical Inhibition During Motor Imagery: An  
689 Adaptive Threshold-Hunting Study. *Neuroscience*, **434**, 102–110.

690 Oldfield, R.C. (1971) The assessment and analysis of handedness: The Edinburgh inventory.  
691 *Neuropsychologia*, **9**, 97–113.

692 Oldrati, V., Finisguerra, A., Avenanti, A., Aglioti, S.M., & Urgesi, C. (2021) Differential  
693 Influence of the Dorsal Premotor and Primary Somatosensory Cortex on Corticospinal  
694 Excitability during Kinesthetic and Visual Motor Imagery: A Low-Frequency Repetitive  
695 Transcranial Magnetic Stimulation Study. *Brain Sciences*, **11**, 1196.

696 Persichetti, A.S., Avery, J.A., Huber, L., Merriam, E.P., & Martin, A. (2020) Layer-Specific  
697 Contributions to Imagined and Executed Hand Movements in Human Primary Motor Cortex.  
698 *Current Biology*, 1–5.

699 Rannaud Monany, D., Lebon, F., Dupont, W., & Papaxanthis, C. (2022) Mental practice  
700 modulates functional connectivity between the cerebellum and the primary motor cortex.  
701 *iScience*, **25**, 104397.

702 Rossi, S., Hallett, M., Rossini, P.M., & Pascual-Leone, A. (2009) Safety, ethical  
703 considerations, and application guidelines for the use of transcranial magnetic stimulation in  
704 clinical practice and research. *Clinical Neurophysiology*, **120**, 2008–2039.

705 Rossini, P., Barker, A., & Berardelli, A. (1994) Non-invasive electrical and magnetic  
706 stimulation of the brain, spinal cord and roots: basic principles and procedures for routine  
707 clinical application. Report of an IFCN. *and Clinical*, **91**, 79–92.

708 Ruffino, C., Papaxanthis, C., & Lebon, F. (2017) Neural plasticity during motor learning with  
709 motor imagery practice: Review and perspectives. *Neuroscience*, **341**, 61–78.

710 Sakai, K., Ugawa, Y., Terao, Y., Hanajima, R., Furubayashi, T., & Kanazawa, I. (1997)  
711 Preferential activation of different I waves by transcranial magnetic stimulation with a figure-  
712 of-eight-shaped coil. *Experimental Brain Research*, **113**, 24–32.

713 Samusyte, G., Bostock, H., Rothwell, J., & Koltzenburg, M. (2018) Short-interval  
714 intracortical inhibition: Comparison between conventional and threshold-tracking techniques.  
715 *Brain Stimulation*, **11**, 806–817.

716 Siebner, H.R. (2020) Does TMS of the precentral motor hand knob primarily stimulate the  
717 dorsal premotor cortex or the primary motor hand area? *Brain Stimulation*, **13**, 517–518.

718 Spampinato, D. (2020) Dissecting two distinct interneuronal networks in M1 with transcranial  
719 magnetic stimulation. *Experimental Brain Research*,.

720 Spampinato, D.A., Celnik, P.A., & Rothwell, J.C. (2020) Cerebellar–Motor Cortex  
721 Connectivity: One or Two Different Networks? *J. Neurosci.*, **40**, 4230–4239.

722 Stinear, C.M., Byblow, W.D., Steyvers, M., Levin, O., & Swinnen, S.P. (2006) Kinesthetic,  
723 but not visual, motor imagery modulates corticomotor excitability. *Experimental Brain*  
724 *Research*, **168**, 157–164.

725 Tanaka, H., Matsugi, A., & Okada, Y. (2018) The effects of imaginary voluntary muscle  
726 contraction and relaxation on cerebellar brain inhibition. *Neuroscience Research*, **133**, 15–20.

727 Tokimura, H., Ridding, M.C., Tokimura, Y., Amassian, V.E., & Rothwell, J.C. (1996) Short  
728 latency facilitation between pairs of threshold magnetic stimuli applied to human motor  
729 cortex. *Electroencephalography and Clinical Neurophysiology - Electromyography and*  
730 *Motor Control*, **101**, 263–272.

731 Van den Bos, M.A.J., Menon, P., Howells, J., Geevasinga, N., Kiernan, M.C., & Vucic, S.  
732 (2018) Physiological Processes Underlying Short Interval Intracortical Facilitation in the  
733 Human Motor Cortex. *Frontiers in neuroscience*, **12**, 240.

734 Volz, L.J., Hamada, M., Rothwell, J.C., & Grefkes, C. (2015) What Makes the Muscle  
735 Twitch: Motor System Connectivity and TMS-Induced Activity. *Cereb. Cortex*, **25**, 2346–  
736 2353.

737 Vucic, S., Cheah, B.C., Krishnan, A. V., Burke, D., & Kiernan, M.C. (2009) The effects of  
738 alterations in conditioning stimulus intensity on short interval intracortical inhibition. *Brain*  
739 *Research*, **1273**, 39–47.

740 Vucic, S., Howells, J., Trevillion, L., & Kiernan, M.C. (2006) Assessment of cortical  
741 excitability using threshold tracking techniques. *Muscle & nerve*, **33**, 477–486.

742 Werhahn, K.J., Fong, J.K.Y., Meyer, B.-U., Priori, A., Rothwell, J.C., Day, B.L., &  
743 Thompson, P.D. (1994) The effect of magnetic coil orientation on the latency of surface EMG  
744 and single motor unit responses in the first dorsal interosseous muscle.  
745 *Electroencephalography and Clinical Neurophysiology/Evoked Potentials Section*, **93**, 138–  
746 146.

747 Wessel, M.J., Draaisma, L.R., Morishita, T., & Hummel, F.C. (2019) The Effects of  
748 Stimulator, Waveform, and Current Direction on Intracortical Inhibition and Facilitation: A

- 749 TMS Comparison Study. *Frontiers in Neuroscience*, **13**, 1–9.
- 750 Yahagi, S. & Kasai, T. (1999) Motor evoked potentials induced by motor imagery reveal a  
751 functional asymmetry of cortical motor control in left- and right-handed human subjects.  
752 *Neuroscience letters*, **276**, 185–188.
- 753 Ziemann, U. (2020) I-waves in motor cortex revisited. *Exp Brain Res*, **238**, 1601–1610.
- 754 Zoghi, M., Pearce, S.L., & Nordstrom, M.A. (2003) Differential modulation of intracortical  
755 inhibition in human motor cortex during selective activation of an intrinsic hand muscle. *The*  
756 *Journal of physiology*, **550**, 933–946.
- 757

758 **Table**

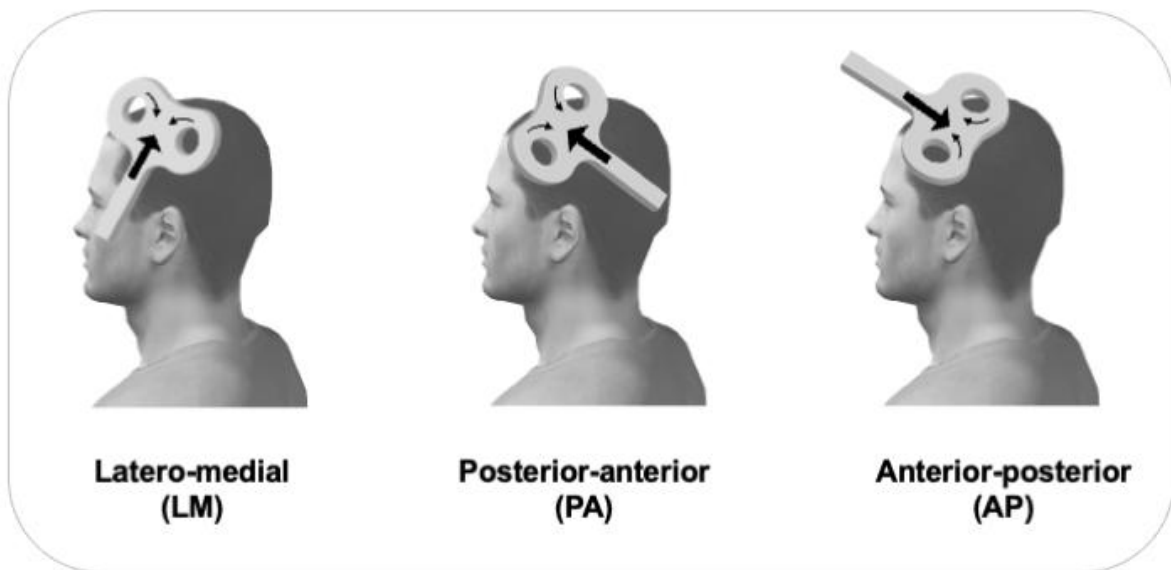
Subject	rMT <sub>PA</sub>	rMT <sub>AP</sub>	aMT <sub>PA</sub>	aMT <sub>AP</sub>	aMT <sub>LM</sub>	MEP <sub>target</sub>
1	40	46	26	35	30	0.213
2	32	41	28	35	29	0.384
3	50	35	28	39	35	0.109
4	46	55	39	48	40	0.095
5	39	51	37	44	44	0.079
6	32	32	25	28	29	0.337
7	45	49	39	41	44	0.291
8	45	56	35	50	35	0.647
9	43	55	33	47	34	0.255
10	30	35	26	30	31	0.234
11	50	52	43	46	43	0.170
12	36	40	27	34	30	0.162
13	35	48	29	42	33	0.258
14	38	42	31	36	34	0.368
15	43	49	34	42	37	0.263
16	40	45	36	41	39	0.313
17	41	49	32	42	35	0.119
<b>Mean</b>	<b>40.3</b>	<b>45.9</b>	<b>32.2</b>	<b>40</b>	<b>35</b>	<b>0.252</b>
<b>SD</b>	<b>6.2</b>	<b>7.6</b>	<b>5.5</b>	<b>6.4</b>	<b>5.2</b>	<b>0.14</b>

759

760 **Table 1:** Individual rMT and aMT expressed in %MSO (Rossini et al., 1994) according  
761 to PA and AP orientations. The individual MEP<sub>target</sub> amplitude (mV) has been calculated  
762 from the mean of 15 MEPs elicited at 115% rMT<sub>PA</sub>.

763

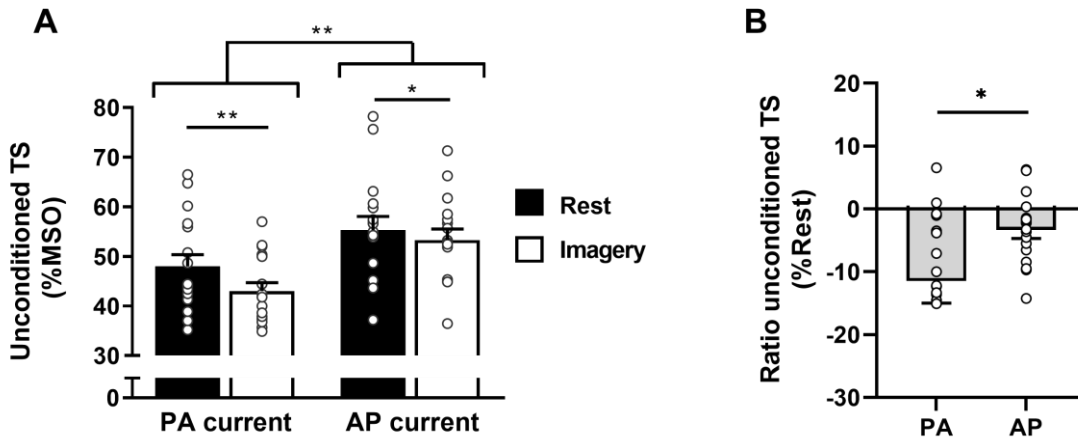
764 **Figures**



765

766 **Figure 1:** Illustration of the coil orientations and their direction of currents induced in  
767 the brain (large arrows) by single- and paired-pulse TMS.

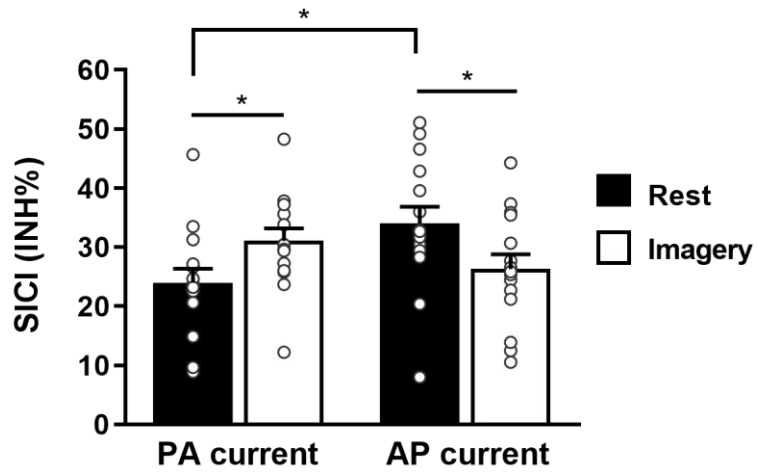
768



769

770 **Figure 2:** **A)** Mean  $\pm$  SE for the unconditioned TS Intensity (%MSO) obtained with the  
 771 hunting-threshold technique at rest and during motor imagery for the two current  
 772 orientations. Lower values of %MSO indicate lower TS intensities to reach the  $MEP_{target}$   
 773 amplitude. **B)** Ratio for the unconditioned TS Intensity obtained during motor imagery  
 774 and expressed as a percentage of rest condition for the two current orientations.  
 775 Negative values indicate lower TS intensities during Imagery compared to rest, and  
 776 therefore, an increase in corticospinal excitability which is greater with PA orientation  
 777 than with AP orientation.  
 778 Data points represent individual participants. PA: posterior-anterior; AP: anterior-  
 779 posterior. \* $p < .05$ ; \*\* $p < .01$ .

780



781

782 **Figure 3:** Mean  $\pm$  SE for the SICI (%INH) obtained with the hunting-threshold  
 783 technique at rest and during motor imagery for the two current orientations.  
 784 Data points represent individual participants. PA: posterior-anterior; AP: anterior-  
 785 posterior. \* $p < .05$

786

787 **Data Accessibility**

788 All datasets will be freely available on the Open Science Framework repository upon  
789 publication at <https://osf.io/ks92r/>

790

791



792 **List of abbreviations**

- 793 AP –Anterior-Posterior
- 794 aMT –active Motor Threshold
- 795 CS –Conditioned Stimulus
- 796 EMG –Electromyographic
- 797 FCR –Flexor Carpi Radialis
- 798 GABA<sub>A</sub> –Gamma-aminobutyric acid type A receptor
- 799 INH –Inhibition
- 800 M1 –Primary Motor Cortex
- 801 MEPs –Motor Evoked Potentials
- 802 MI –Motor imagery
- 803 MSO –Maximum Stimulator Output
- 804 MVC –Maximal Voluntary Contraction
- 805 PA –Posterior-Anterior
- 806 PMd –dorsal Premotor cortex
- 807 RMS –Root Mean Square
- 808 rMT –resting Motor Threshold
- 809 SICI –Short-Interval Intracortical Inhibition
- 810 TS –Test Stimulus
- 811 TMS –Transcranial magnetic stimulation